European Journal of Radiology 114 (2019) 14–24

Contents lists available at ScienceDirect

European Journal of Radiology

journal homepage: www.elsevier.com/locate/ejrad

Review

The present and future of deep learning in radiology

Luca Saba[a], Mainak Biswas[b], Venkatanareshbabu Kuppili[b], Elisa Cuadrado Godia[c], Harman S. Suri[d], Damodar Reddy Edla[b], Tomaž Omerzu[e], John R. Laird[f], Narendra N. Khanna[g], Sophie Mavrogeni[h], Athanasios Protogerou[i], Petros P. Sfikakis[j], Vijay Viswanathan[k], George D. Kitas[l,m], Andrew Nicolaides[n,o], Ajay Gupta[p], Jasjit S. Suri[q,*]

[a] Department of Radiology, Policlinico Universitario, Cagliari, Italy
[b] National Institute of Technology Goa, India
[c] IMIM – Hospital del Mar, Passeig Marítim 25-29, Barcelona, Spain
[d] Brown University, Providence, RI, USA
[e] Department of Neurology, University Medical Centre Maribor, Slovenia
[f] Cardiology Department, St. Helena Hospital, St. Helena, CA, USA
[g] Cardiology Department, Apollo Hospitals, New Delhi, India
[h] Cardiology Clinic, Onassis Cardiac Surgery Center, Athens, Greece
[i] Department of Cardiovascular Prevention & Research Unit Clinic & Laboratory of Pathophysiology, National and Kapodistrian Univ. of Athens, Greece
[j] Rheumatology Unit, National Kapodistrian University of Athens, Greece
[k] MV Hospital for Diabetes and Professor M Viswanathan Diabetes Research Centre, Chennai, India
[l] Arthritis Research UK Centre for Epidemiology, Manchester University, Manchester, UK
[m] Department of Rheumatology, Dudley Group NHS Foundation Trust, Dudley, UK
[n] Vascular Screening and Diagnostic Centre, London, UK
[o] Department of Biological Sciences, University of Cyprus, Nicosia, Cyprus
[p] Brain and Mind Research Institute and Department of Radiology, Weill Cornell Medical College, NY, USA
[q] Stroke Monitoring and Diagnostic Division, AtheroPoint™, Roseville, CA, USA

ARTICLE INFO

Keywords:
Deep learning
Machine learning
Medical imaging
Radiology

ABSTRACT

The advent of Deep Learning (DL) is poised to dramatically change the delivery of healthcare in the near future. Not only has DL profoundly affected the healthcare industry it has also influenced global businesses. Within a span of very few years, advances such as self-driving cars, robots performing jobs that are hazardous to human, and chat bots talking with human operators have proved that DL has already made large impact on our lives. The open source nature of DL and decreasing prices of computer hardware will further propel such changes. In healthcare, the potential is immense due to the need to automate the processes and evolve error free paradigms. The sheer quantum of DL publications in healthcare has surpassed other domains growing at a very fast pace, particular in radiology. It is therefore imperative for the radiologists to learn about DL and how it differs from other approaches of Artificial Intelligence (AI). The next generation of radiology will see a significant role of DL and will likely serve as the base for augmented radiology (AR). Better clinical judgement by AR will help in improving the quality of life and help in life saving decisions, while lowering healthcare costs.

A comprehensive review of DL as well as its implications upon the healthcare is presented in this review. We had analysed 150 articles of DL in healthcare domain from PubMed, Google Scholar, and IEEE EXPLORE focused in medical imagery only. We have further examined the ethic, moral and legal issues surrounding the use of DL in medical imaging.

Abbreviations: ANN, artificial neural network; cIMT, carotid intima-media thickness; CNN, convolution neural network; CT, computed tomography; DBN, deep belief network; DL, deep learning; ELM, extreme learning machine; FCN, fully connected network; FLD, fatty liver disease; GPU, graphics processing unit; LI, lumen-intima; MA, media adventitia; ML, machine learning; MLP, multi-layer perceptron; MRI, magnetic resonance imaging; RNN, residual neural network; TC, tissue characterization

* Corresponding author.
E-mail address: jasjit.suri@atheropoint.com (J.S. Suri).

https://doi.org/10.1016/j.ejrad.2019.02.038
Received 23 September 2018; Received in revised form 17 February 2019; Accepted 26 February 2019
0720-048X/

1. Introduction

The idea of machine learning (ML) takes inspiration from the initial work done on the cat's visual cortex by Hubel and Wiesel [1]. The visual depiction of visual cortex was earlier thought to be a holistic process, but was found to be hierarchical (explained later). This discovery led to the foundation of artificial neural networks (ANNs) [2] and subsequently deep learning [3]. In the Fig. 1, the human brain is represented as a hierarchical network of neuron layers. The neurons do the computation on input data from lower layer neurons and pass output to other higher layer neurons through the network. There are five basic layers of neurons: primary visual cortex (V1), secondary visual cortex (V2), V4, inferotemporal cortex (IT) posterior and IT-anterior layer of neurons as shown in Fig. 1. The lower level neurons (shown in Fig. 1) in the V1 detects basic features such as border line features of objects or edges. The V2 neurons encode these elementary features into junctions of lines to create basic visual features. The V4 layer neurons detect more complex combinations of these features. The IT posterior neurons detect and recognize entire object shapes (such as face) over a wide range of locations, sizes, and angles as shown in Fig. 1. The IT-anterior neurons form a more abstract or semantic meaning about the visual information. The first worthwhile implementation of this knowledge was in the form of weighted single-layer artificial neural network called perceptron [4]. The perceptron is a single-layer network capable of binary classification, such as low or high risk. It works by drawing a boundary between the two classes of features. The process of drawing boundary based on known examples (whose outputs are known) is called training. It applies a greedy approach of finding the first best-fitting boundary which separates the classes by changing the weights of the neurons in the first layer in an iterative fashion. These weights are just like the coefficients of linear equation (an equation in which there are terms of degree one and having the coefficients to these terms) which resolves by changing itself iteratively until it reaches the solution point. It is reached if the error or the difference between the desired and the actual output of the perceptron becomes zero for all training samples. The accuracy is checked by testing the trained perceptron on unknown examples (whose outputs are unknown). Note that perceptron will succeed only when the two classes are linearly separable [5]. For classes which are not linearly separable, the solution is mapped to a non-linear separation by introducing a hidden layer between the input and output layers [6] (discussed later), also called multi-layer perceptron (MLP). Other similar examples of single-layer neural networks developed during this period were Radial Basis Neural Network [7], Support Vector Machines [8], and Extreme Learning Machine [9]. The learning laws used for training of single- or multi-layer perceptron were categorized into two groups i.e., error correction rules and gradient rules [10]. The error (between desired and actual output) correction rules used is linear error measure to reduce error at the output while in the gradient rules, the weights of a network were altered with an objective of reducing mean-squared error. In this regard, back propagation algorithm developed by Hinton et al. [11], is an important landmark in the field of learning laws which had the ability of quick generalization. In the field of radiology, the contribution of ML for classification of the disease severity and organ segmentation (or segregation) has been significant. Examples of classification framework include detection of fatty liver disease from liver ultrasound images [12–14], or ovarian cancer detection and risk stratification from ultrasound images [15–17], or stroke risk stratification using carotid ultrasound [18,19]. Example of segmentation in radiological images include: carotid artery segmentation from ultrasound images for carotid intima- media thickness and lumen segmentation [20–22], plaque characterization from CT images [23], brain segmentation from MR images/volumes [24] and left ventricle segmentation [25] from MR images.

Up to now, the strategy followed for image classification or segmentation was similar: extract features from images using feature extraction algorithm, selection of best features, if the number of features are large, and then application of the machine learning algorithms to transform the online features by the offline training coefficients to either classify the tissues or delineate the components of the images as part of segmentation. This effectively translates to the functionality and processing of human brain's neural responses to the different visual stimuli [26,27]. Experiments by Kay et al. [28] showed that Gabor [29] filters or their variations can explain the responses of primary visual cortex of human subjects but not further. This so happens because neurons at lower levels respond to simple lines at different angles *i.e.*, perceptron. As the number of hidden layers increases (the network becomes **Deeper**), the higher level neurons respond to complex relationships between features *i.e.*, lines which are perpendicular to each other. This also encompasses the hierarchical learning in a gist of the visual cortex as already shown in Fig. 1.

An important milestone in transforming the machine learning to deep learning was achieved by Krizhevsky et al. [30] during implementation of ImageNet in 2012. The authors proposed a DL [31] model *i.e.*, AlexNet that achieved 15.2% top-5classification error (Err) while segregating 1.2 million high-resolution images in 1000 different classes. AlexNet was the first deep learning model (five layer deep network (CNN) [31] (discussed later) to be applied in the ImageNet challenge. Since then, the error has been reduced remarkably to 2.25% recently ([32–36]) with the number of deep layers increasing each year. Each DL model and their error rate are given in Table 1.In this review, we have collected information on current research on DL applications in several fields such as genomics, imaging and signal processing. Initially, we looked used the keyword “deep learning”, “convolution”, “healthcare” using search engines such as Google Scholar, ScienceDirect, PubMed, SCOPUS and IEEE databases, however this search was inconclusive as it opened up almost all deep learning related works. We therefore modified our search terms to include image modalities such as “MRI”, “CT”, “Ultrasound” etc and specific keywords such as “DNA sequencing”, “gene”, etc. We segregated the relevant research outputs

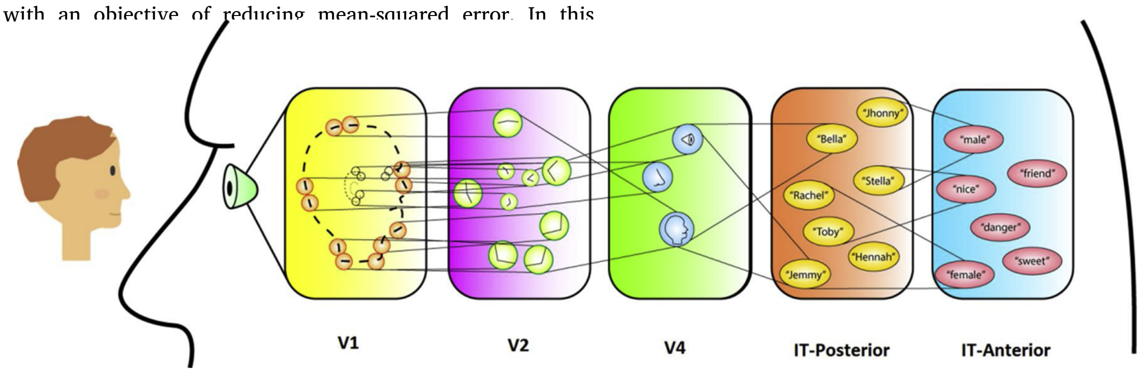

Fig. 1. A neural network representation of human brain (image courtesy: https://grey.colorado.edu/CompCogNeuro/index.php/CCNBook/Perception).

Table 1
DL models and their performances.

SN.	Model Name	Year	Top-5 Err* (%)
1	AlexNet [31]	2012	15.3%
2	VGG16 [33]	2014	7.30%
3	GoogleNet [34]	2015	3.58%
4	ResNet [35]	2016	3.57%
5	Squeeze-and-Excitation [36]	2017	2.25%

* Top-5 error rate is the fraction of test images for which the correct label is not among the five labels considered most probable by the mode.

as per the type of modality i.e., “MRI”, “CT”, “DNA sequencing” etc. Inside each segregated class, we further categorized each paper as their organ or disease type. This search went on iteratively bimonthly. We had collected over 150 articles during this process. We focused on medical imagery in the deep learning paradigm for the review paper and selected few papers published recently based on organ types to assess the work done in various physiologies.”

There are several key differences between ML and DL methodologies. The DL methods learn high-level representations of the data using multilayer computational models which are useful in organ segmentation or disease classification in images. Conventional models such as ANNs require pre-processing and input clinical ground truth yielding radiological feature extraction whereas, DL, allows the algorithm to automatically learn features from raw and noisy data and therefore helps in superior training and subsequently superior learning. It does so by using the concepts of dimensionality reduction (compression of images), non-linearity (variations in the intensity distribution).

DL optimizes feature engineering process to provide the software classifier with the information that maximizes its performance with respect to the final task leading to its superior training. DL models are capable of extraction of highly complex, nonlinear dependencies from raw data which is responsible for superior training. Due to increase in volume of raw datasets, DL models can be used in jointly learning from a combination of datasets, without worrying about the commonality or discord of features. DL can be used for multi-task learning *i.e.*, using the same data for different purposes, such as, both disease classification and organ segmentation [37]. The DL explains the neural response to visual stimuli for the entire visual cortex of the human brain [38–40]. This particular property enables DL models pre-trained on a particular subject while to be tested on different subjects if the features of the training and test subjects have similar cortical representation [41,42]. This particular feature of DL is also called Transfer Learning (TL) [43] and is highly popular in ML and DL community [44–46]. In this regard, a comprehensive review on DL applications in medical imaging was recently attempted [47]. The review covers different kinds DL models applied in different imaging modalities. Almost 300 articles have been covered. However, an intrinsic understanding of the DL models applied in medical imaging from the point of view of medical professionals is lacking. In this review we have tried to address this issue in the next subsection.

DL like ML can be categorized into two types: supervised and unsupervised. Supervised learning deals with labelled data while unsupervised learning deals with unlabeled data. The machine tries to learn interrelationships between data elements. The most popular DL supervised learning models are currently convolution neural networks (CNN) and residual neural network (RNN). Deep Belief Networks (DBN) and Autoencoders are most popular unsupervised learning models. CNN has been used for both medical image characterization [48,49] and segmentation [50,51]. RNNs have been used for characterization till now [35]. Although DBN is used for unsupervised learning it has been implemented for segmentation [52]. The DL model of autoencoder has been used for both characterization [53,54] and segmentation [55,56]. This representation is diagrammatically shown in Fig. 2. CNN [31] is the most popular DL model for medical imaging. It follows the same principle of hierarchical feature learning of the visual cortex. However, it uses convolution [57] filters in place of weights for its functioning. This convolution operation is diagrammatically shown in Fig. 3. A convolution filter is a matrix of weights which does a point-wise multiplication across the whole image to create neural map or feature map of the image. The CNN applies several convolution filters to create feature maps of the original image which represent its hidden layers. These feature maps are down sampled representations of the original image. Further, these feature maps are worked upon layer by layer to extract high level features. From this point on we will call “hidden layers” as "deep layers". Pooling is applied to these feature maps for dimensionality reduction and extraction of important features. The deep layers of CNN are shown in Fig. 4. This process is repeated creating more deep layers and thus increasing the depth of the network. Finally, an MLP is applied for disease classification This MLP is also called a fully connected network (FCN) in the context of CNN. While the entire body of CNN is related to features, extracted in form of feature maps, the FCN is the final piece at the end of CNN where the classification takes place. Initially the CNN along with FCN weights learn from training data based on the ground truth information. The FCN takes the deep features produced from the deep layers as input to produce the classification output for test data. CNNs allow segmentation too. In the case of segmentation, FCN is not used. The extracted features from the last layers of CNN are either up sampled or the convolution process is reversed to generate segmentation maps [58,59]. The flexibility of CNN for both characterization and segmentation has made CNN the most popular DL model. In this work, the DL application examples discussed later are some form of CNN. Autoencoders [60] are a class of DL models used for unsupervised learning of data where the target values are actually the inputs. There are two paths in an autoencoder: encoder and decoder. The encoder compresses the image data while the decoder expands it. There are several hidden layers for encoder and same number of layers for decoder. Due to compression and expansion of the image within the autoencoder, the intermediate hidden layers learn complex interrelationships of pixels within an image. The learning of this representation is useful while reconstructing images, clearing noise from image or using it for segmentation or image registration. An example of working is training the autoencoder to denoise a corrupted input image (denoising autoencoder [61]). Residual neural network (RNN) [35] is also gaining popularity in disease classification in radiology images. An RNN functions by learning the extra residual features between a high level and lower level deep layers. This helps in preventing accuracy saturation even if network becomes deeper. Deep Belief Network (DBN) [62] is another example unsupervised deep neural network which is trained layer-by-layer to reduce reconstruction error. The detailed working of each model is provided [63].

DL algorithms suffer from over-fitting and under-fitting. Over-fitting happens if the input medical image used for training the DL is corrupted or very noisy and the weights fit exactly to characterize the existing training data and fail to characterize test data. In underfitting, the training images does not cover entire spectrum and hence the training of neurons does not generalize to identify test images. Over-fitting and under-fitting leads to faulty training of the DL-based system. ML algorithms too suffer from this phenomenon. One way is regularization where a penalty term is added to the loss function to penalize terms of high order and magnitude (outliers or noise) [64]. This reduces the training error. DL systems generally apply dropout strategy where few network connections are dropped to prevent over-fitting [31].

In the next few sections we will deal with present and future scenarios of DL in radiology, potentialities of DL in radiology, risks of DL, and finally the conclusion.

2. The present state of deep learning-based radiology

Within a very short period of time, DL has taken center stage in the field of medical imaging. In this portion we will review a sampling of

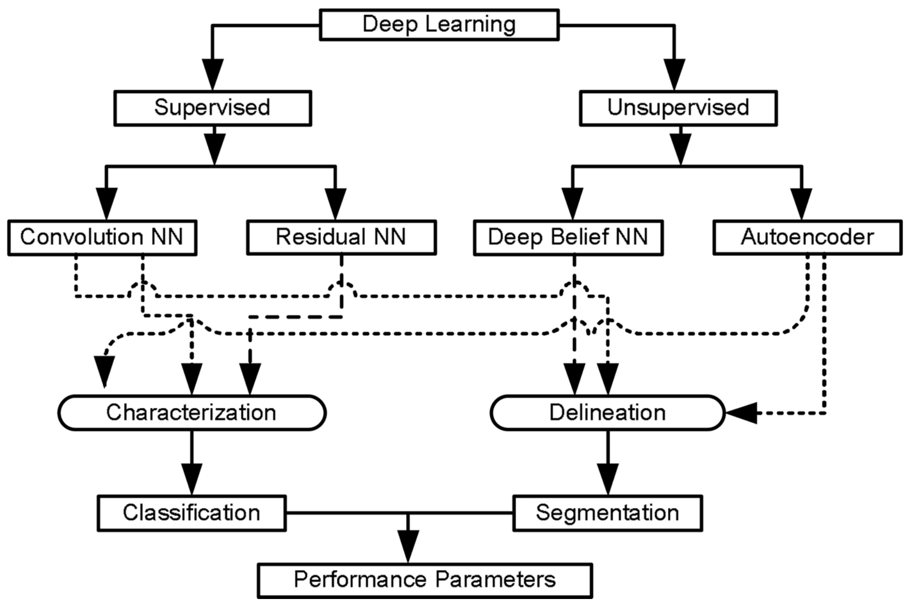

Fig. 2. Categorization of DL models and their applications in image characterization and segmentation.

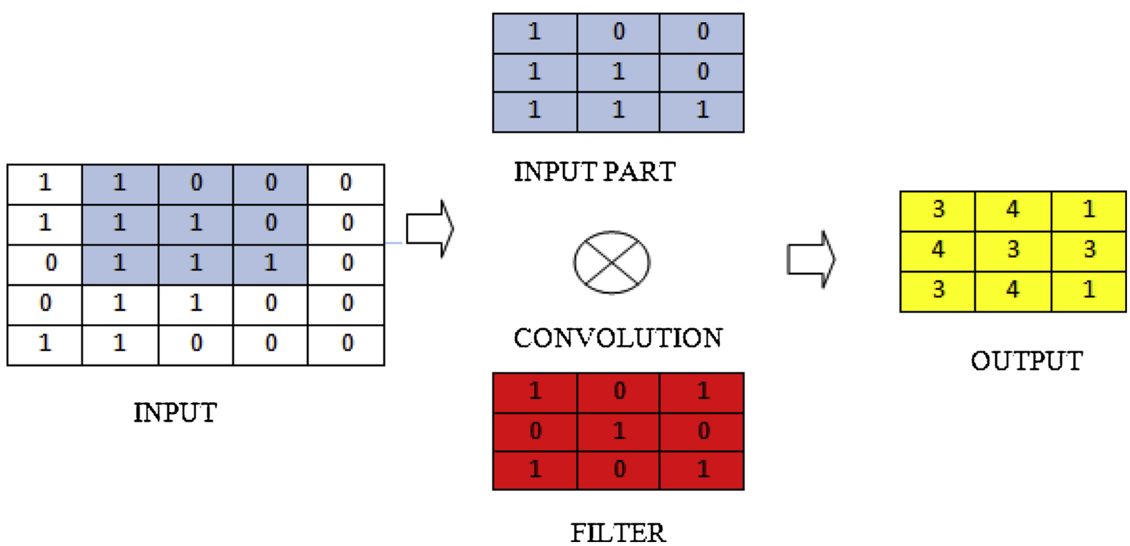

Fig. 3. Convolution operation.

recent literature in DL as it applies to the practice of radiology. This section gives an overview of different image modalities for different organs of human body. We have provided one DL application in Hepatology, Cardiology, Neurology, Urology and Pulmonology. They are given as follows:

2.1. An application in Hepatology for Fatty liver disease risk stratification

In the past few years DL researchers have shown considerable interest in stratification of liver diseases, segmentation of liver and liver lesions from radiological images. In this regard, Hu et al. [65] proposed DL model for segmentation of liver from CT images. Li et al. [66] proposed a DL model for liver tumor segmentation from CT images. This work was a significant step in diagnosis of liver cancer. Recently, considerable research efforts has been applied in the area of classification of liver diseases from radiological images. Fatty liver disease (FLD) is one of the major causes of death among the USA adult population (aged 45–54 years) [67]. Early diagnosis and treatment will save countless lives over few years. In this respect Biswas et al. [68] developed a DL model for tissue characterization (TC) of FLD from liver ultrasound images shown in Fig. 5. The DL model used for characterization is 22 deep layer-ed CNN with special layers called inception layers [69].

The inception layer is a combination of multiple convolution filters applied in a single layer (the convolution filters have been addressed before while discussing CNN). Therefore, inception layer is used to perform multiple convolution operations in a single layer which helps in quick convergence and generalization without increasing depth and complexity of the DL model. The accuracy achieved using the DL model was 100% for 10- fold cross-validation.

2.2. Cardiology application for medial thickness segmentation and cIMT measurement

Stroke or heart attack due to vascular atherosclerosis affects 10 million people worldwide, with fatalities accounting for five million people [70]. In-time diagnosis and medication can mitigate the risk of CVDs. In this respect, a two-stage DL-based system was proposed by Biswas et al. [71] for cIMT measurement. The first stage DL is used for feature extraction. It consists of 13 deep layers which extracts features

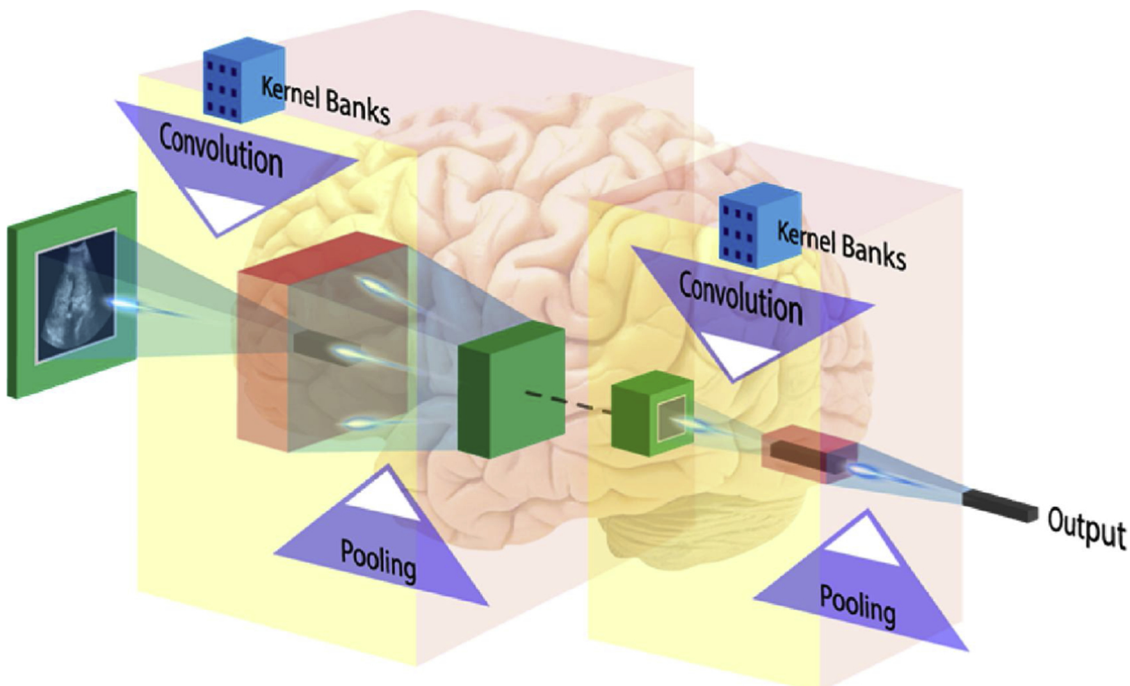

Fig. 4. Convolution Neural Network (Courtesy of AtheroPoint, CA, USA).

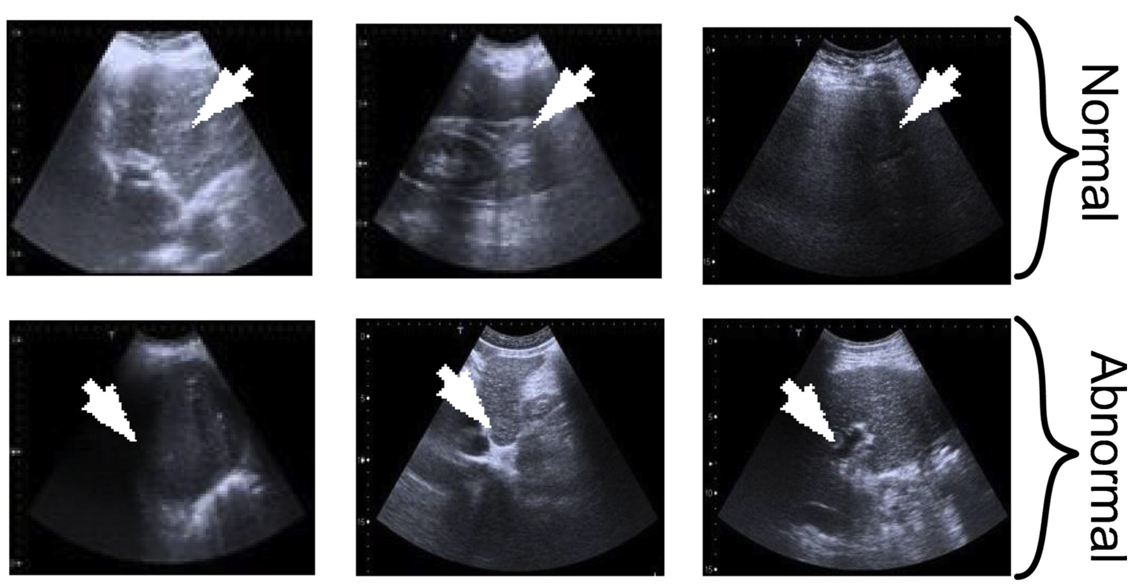

Fig. 5. Fatty Liver Disease US images (Normal Liver: Upper Row, Abnormal: Lower Row (image courtesy: AtheroPoint™)) (Courtesy of AtheroPoint, CA, USA).

from the images. However, unlike other CNN it does not apply FCN at the end for classification. Instead, it uses upsample layers for the features extracted from the first stage and upsample them in the second stage.

These upsampled features [72] form the segmented output of the original image. For this task, two radiologists were employed for tracing lumen-intima (LI) and media adventitia (MA) borders. These tracings form the gold standard of the experiment. The original images were divided into two parts: 90% training and 10% testing. The training images along with their gold standard was fed into the system for training, twice: the first time for learning to segment the LI from the tissue, the second time for learning to segment the MA wall. Once learnt, the test images were segmented. The LI and MA borders were delineated and cIMT was computed for the test images. For, this experiment 396 B-mode ultrasound images of left and right carotid artery was taken from 203 patients. The readings showed an overall improvement of 20% over the sonographer readings. The six sub-images can be seen in Fig. 6, which show low, medium and high risk patients demonstrate the working of the DL-based system. The red and green lines correspond to the LI and MA border drawn by the DL-based system and the corresponding yellow dotted lines denote the gold standard tracings.

2.3. Neurological application for effective treatment in MR-based Acute Ischemic Stroke

In order to treat patients with AIS, it is a necessity to find the volume of salvageable tissue. This volume assessment is based on fixed thresholds and single imaging modalities. A deep CNN model (37 deep layers) [73] using nine MR image biomarkers was trained to predict

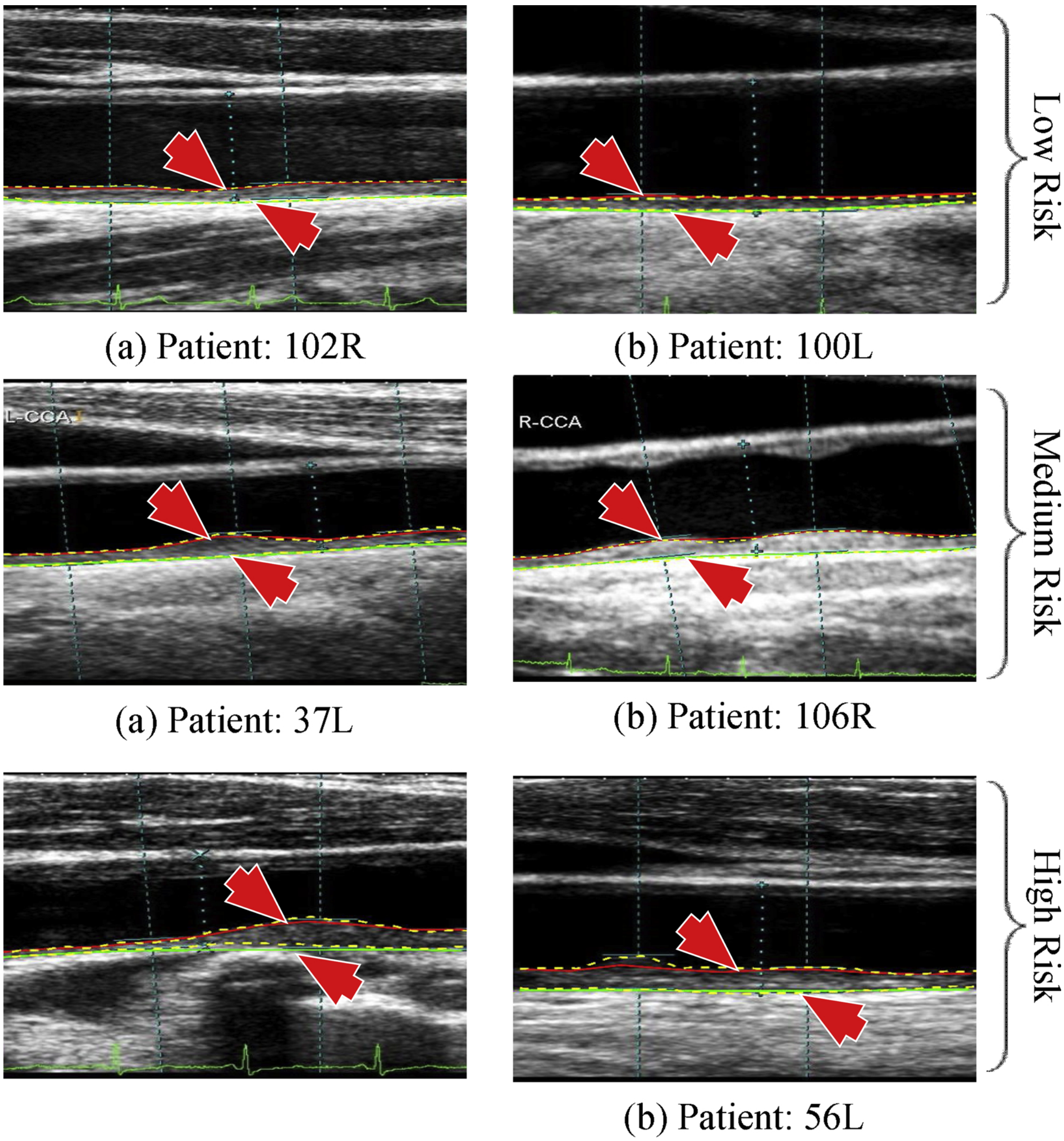

Fig. 6. LI- and MA- border by the DL-based system shown in red (arrows at 5 o' clock) and green (arrows at 11 o' clock). Gold standard tracings are shown in dotted yellow. Top row corresponds to low risk, middle row denotes medium risk and bottom row signifies high risk patients. The cIMT error analogous to the two gold standards was found to be 0.126 ± 0.134 mm and 0.124 ± 0.100 mm, respectively. The lumen-intima (LI) error with respect to the two gold standards was found to be 0.077 ± 0.057 mm and 0.077 ± 0.049 mm, respectively. The media-adventitia (MA) error corresponding to the two gold standards were 0.113 ± 0.105 mm and 0.109 ± 0.088 mm, respectively (image courtesy: AtheroPoint™) (Courtesy of AtheroPoint, CA, USA).

final imaging outcome. Its performance was compared with two other CNN model. The first is CNN of two convolution layers using nine MR image biomarkers and the other is a Tmax CNN (two layers) based on Tmax [74] biomarker. For this experiment, 222 patients were selected. Out of them, 187 were treated with recombinant tissue-type plasminogen activator (rtPA). All patients were scanned after symptom onset in the follow-up. The results are shown in Fig. 7. It is seen that the deep CNN model gave better visual output then the other CNN models. It shows that deeper (more number of deep layers) models give a better output than shallow models. Among two patients A and B, patient A (age: 58 years) gave no signs of visual lesions which was correctly predicted by deep CNN model while the other models over predicted. For patient B (age: 44 years) deep CNN prediction is more accurate. While comparing performance, deep CNN had better area-under-curve (AUC) of 0.88 ± 0.12 compared to shallow CNN (AUC: 0.85 ± 0.11) and Tmax CNN (AUC: 0.72 ± 0.14).

2.4. An application in urology for prostate cancer diagnosis

A patch-based Deep-CNN model is proposed to classify prostate cancer (PC) and non-cancer (NC) image patches from multiparametric MR images [75]. In this experiment, the MR image data was collected from 195 patients and images were aligned and resampled to high resolution images. A radiologist with 11 years of experience was employed to label PC and NC zone in the images and draw a region-of interest (ROI) around them. The images were pre-processed and augmented using rotation, random shift, random stretching and horizontal flip. This was done to increase the dataset size as the patient's cohort was small. Such physical operations also enable DL models to uncover important features within the data. The ROI patch was extracted from all the images. Finally, 159 patients' data (444 ROIs: 215 PC/229 NC) was used for training, 17 patients' data (48 ROIs: 23 PC/25 NC) was used for validation and finally 19 patients' data (55 ROIs: 23 PC/32 NC)

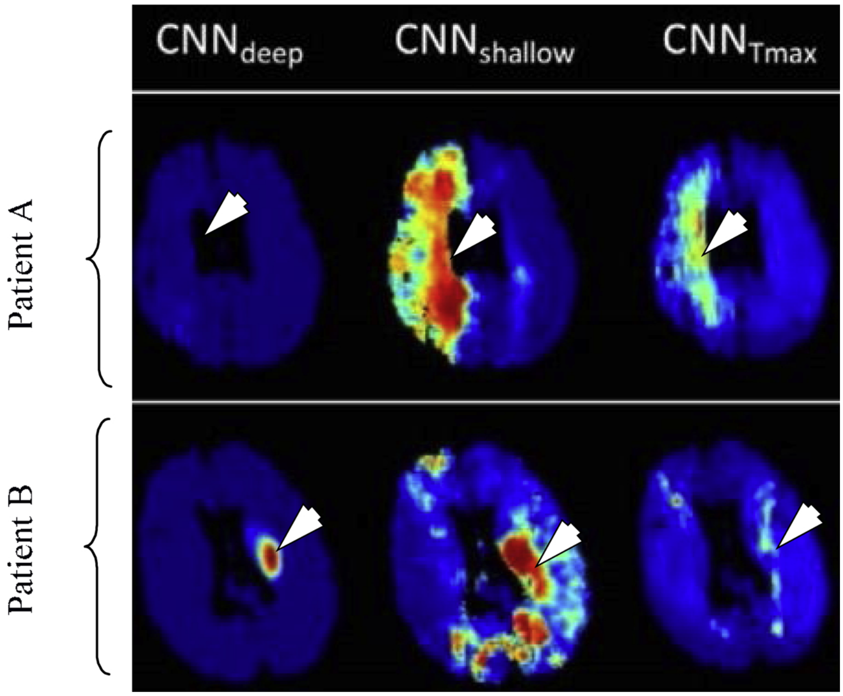

Fig. 7. DL output results from follow-up scan on Patient A (Age: 58, male) and Patient B from Deep CNN, Shallow CNN and TmaxCNN (lesions pointed to by arrows at 7 o' clock). Patient A (Age: 44, male) is correctly predicted as having no lesions by Deep CNN while over-predicted by Shallow CNN and Tmax CNN. Patient B is correctly predicted by all the CNN model. However prediction of Deep CNN is better (Reprinted with permission of the American Thoracic Society. Copyright [73])).

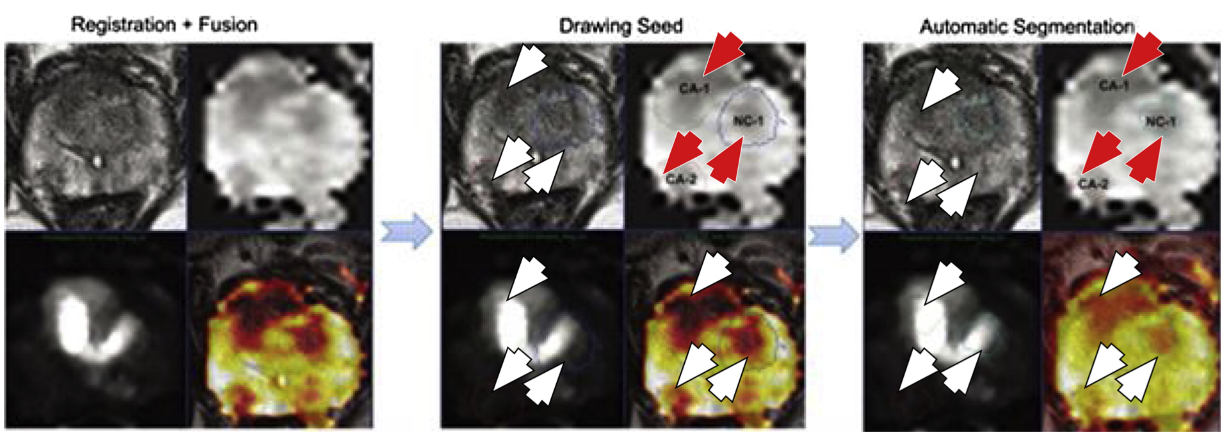

Fig. 8. Outputs of registration, pre-processing and placement of ROI. The images used were T2-weighted, diffusion-weighted, and apparent diffusion coefficient images. Lesions in the images are marked by WHITE arrows. Lesions are later characterized by radiologists. CA ROIs are pointed to by RED arrows at 7 o' clock while NC ROIs pointed to by arrows at 1 o' clock. (**Permission Pending** [75]).

for testing. The Deep CNN model consisted of three blocks followed by a FCN layer. Each block contained three deep layers. The diagnostic accuracy for the test data was in the form of AUC value was 0.944. The outputs of each step are shown in Fig. 8.

2.5. A Pulmonology application for respiratory disease prognosis using CT

A DL study was conducted on CT images on chest to classify patients having chronic obstructive pulmonary disease (COPD) or not. This study was also poised to predict acute respiratory disease (ARD) events and mortality [76]. The dataset consisted of 7983 COPD Gene participants for training and 1000 COPDGene [77] and 1672 ECLIPSE (Evaluations of COPD Longitudinally to Identify Predictive Surrogate Endpoints) [78] participants for testing. The DL structure consisted of three deep layers [31]. The c-statistic for the detection was 0.856. The overall c-statistic for COPDGene and ECLIPSE datasets was 0.64 and 0.55, respectively. The outputs for each f the three layers of the DL model is shown in Fig. 9.

3. Future of deep learning

3.1. DL in radiology

The impact of DL in industry has been huge [79–90]. The next big leap of automation using DL is happening in the field of radiology. It is evident from the fact that maximum publication with respect to DL in healthcare is happening in medical imaging [91]. The presence of open source software [92–94] has made it possible for researchers and scientist community to build DL tools with relative ease. One possible reason for DL success story is lowering of costs of computer hardware and GPUs [95,96] due to large gaming industry. The usage of GPUs by DL has brought down the computational time which has led to quick training and generalization of the DL models. DL has been used in disease classification [97,98], brain cancer classification [99–101], organ segmentation [102–108], haemorrhage detection [109,110], tumor detection [111–116] are some key progresses. All methodologies showed increase in accuracy then conventional methods.

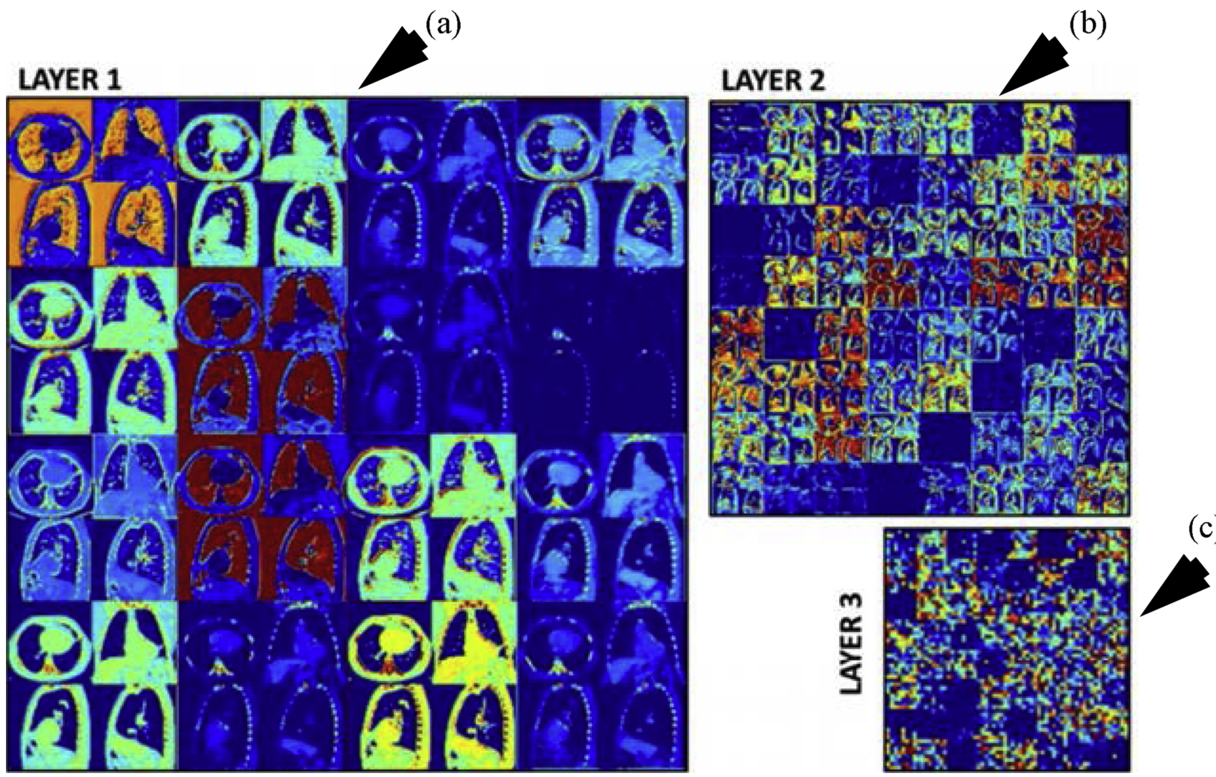

Fig. 9. The outcomes of the three layers (pointed to by arrows at 7 o' clock) of the DL model. Layer 1 output: arrow (a); Layer 2 output: arrow (b) Layer 3 output: arrow (c) (**reproduced with permission**).

3.2. Radiology's future

DL is going is likely to advance medical imaging sciences in the upcoming future. Hospitals and diagnostic centres are needed to upgrade their infrastructure and develop their labs. Medical facilities worldwide must share their databases without compromising the privacy of patients. These databases must be made available for better training of the DL models. The quick processing of image data and availability of reports would enable medical professionals of the future to make a better and timely medical decision-making. This would help in real time treatment of patients and help in saving lives. Overall, the usage of DL in radiology has the potential to improve the health of individual and the wellbeing of society.

4. The future prospective of radiology using deep learning

4.1. Economy

A radiologist can analyse an average of 200 cases a day [117]. A powerful tool such as DL can help radiologists to make accurate decisions in short period of time thus helping him to improve quality of patient's health and growing the volume at the same time – both locally and remotely (such as telemedicine [118]).

In the US, 260 million images are processed everyday including ultrasound, MR and CT images. A hospital can invest 1000 US dollars in their computational systems to process that many images [119] in a day. This would decrease the delay in treatment and lower the medical costs. It is also forecasted that the computer aided diagnosis (CAD) market powered by DL will generate revenue of 1.9 billion US dollars [120] by 2022.

4.2. Augmented radiology and DL

As human drivers may become redundant with the arrival of driverless cars, people are talking about replacement of radiologists by DL systems backed up by billion dollar medical imaging companies such as GE and IBM. However, the hybridization of machine and human intelligence will lead to better prediction model e.g., it has been observed that in a stable, controlled environment statistical models such as DL will be at least as good as, if not better than humans. In real time, however, the environment may change rapidly, data may become noisy, and patterns will become difficult to read. In such situations the statistical models may not work properly or even may fail to give accurate predictions. In such situations, collective intelligence of both man and machine will likely be necessary to better prediction accuracy. Therefore, consensus-based models are needed to be built with equal participation from both man and machine to develop a better hybrid prediction model. The value of human intelligence may actually increase where automation is not possible. The application of DL in radiology will lead to an augmentation of the radiologist's capabilities, by combining technology with human intelligence [121–124].

Radiologists are also going to benefit from applications of DL in picture archiving and communication system (PACS) [125]. DL implementation in PACS will make the availability of images faster, reliable and more accurate.

4.3. Further development of DL

It is predicted that DL will aid in the performance of routine and mundane tasks in radiology while the human will use higher decision-making to render final judgements. The main features in medical diagnosis and prediction using DL techniques will make the consultation to be more interactive between patients and doctors. This will happen as the DL systems will be able to provide evidence when clinical decision to be made is under uncertainty. DL has the potential to develop an ecosystem where medical services will be provided round the clock taking all data into consideration *i.e.*, radiology, patient history, bioinformatics, clinical radiological trials such as retrospective, prospective or longitudinal. This will lead to better patient care.

5. Challenges and risks in deep learning

There are several ethical and moral concerns with regards to implementation of AIDL in clinical diagnosis process. This can be divided into three categories: safety, privacy and morality.

5.1. Safety

Medical professionals are guided by the code “first, do no harm”. AI systems, if employed, will be responsible for safeguarding patients at their most vulnerable state, with no room for preventable error. Medical regulatory bodies should ensure that DL systems are employed following stringent rules ensuring that they are highly robust and accurate. Safety standards should also be time tested and be highly reliable.

5.2. Privacy

DL requires training imaging databases. This will require patient information to be stored in some secure server. Any breach in security will lead to loss of privacy of data. Precautionary measures should be taken and laws should be in place to protect the privacy of patients before allowing DL. Data transmission protocols must be tightly secured and only transmitter or receiver of the image data can truly extract the image information only if they possess the authority.

5.3. Legality

There is a legal issues related with application of DL technologies in healthcare. The foremost is to whom legal liability should be assigned if DL makes a wrong judgement. It is possible that the solution may involve some shared liability between the human authority responsible for design of the DL model and the physician overseeing the application of a given DL technology.

6. Conclusion

In this study we had a broad overlook over the various facets of DL in the field of radiology. We reviewed the concept of DL, its evolution, and presented various DL applications in radiology. We briefly stated the present scenario regarding application of DL in radiology. We also outlined the future potential and its risks in DL pertaining to health care. When properly utilized, DL has the potential to increase the value to the radiologist in the delivery of healthcare by improving patient’s outcomes while reducing costs.

Funding

This research did not receive any specific grant from funding agencies in the public, commercial, or not-for-profit sectors.

Conflict of interests

The authors declare they have no conflict of interests.

Acknowledgement

The authors would like to thank DEITY, Govt. of India, for providing support for carrying out this work under Visvesvaraya Scheme.

Appendix A

In this review, we have collected information on current research on DL applications in several fields such as genomics, imaging and signal processing. Initially, we looked using the keyword “deep learning”, “convolution”, “healthcare” using search engines such as Google Scholar, ScienceDirect, PubMed, SCOPUS and IEEE databases, however this search was inconclusive as it opened up almost all deep learning related works. We therefore modified our search terms to include imaging modalities such as “MRI”, “CT”, and “Ultrasound”. Within MRI, different variants of MRI were searched: magnetic resonance spectroscopy and functional MRI. Similarly for CT, positron emission tomography (PET), single-photon emission computed tomography (SPECT), and contrast CT. Further, different versions of ultrasound were also searched i.e., Doppler, A-mode, B-Mode ultrasound generalized ultrasound. Specific keywords were tried, such as translational bioinformatics, medical imaging, pervasive sensing, medical informatics and public health. We segregated the relevant research outputs as per the type of modality i.e., “MRI”, “CT”, and “Ultrasound”. Inside each segregated class, we further categorized each paper as their organ or disease type. This search went on iteratively bimonthly. We had collected over 150 articles during this process. We focused on medical imagery in the deep learning paradigm for the review paper and selected few papers published recently based on organ types to assess the work done in various physiologies.”

References

[1] David H. Hubel, T.N. Wiesel, Shape and arrangement of columns in cat’s striate cortex, J. Physiol. 165 (3) (1963) 559–568.
[2] Nasser M. Nasrabadi, Pattern recognition and machine learning, J. Electron. Imaging 16 (4) (2007) 049901.
[3] Ian Goodfellow, Yoshua Bengio, Aaron Courville, Yoshua Bengio, Deep Learning Vol. 1 Cambridge MIT press, 2016.
[4] Frank Rosenblatt, The perceptron: a probabilistic model for information storage and organization in the brain, Psychol. Rev. 65 (6) (1958) 386.
[5] Simon Haykin, Neural Networks, a Comprehensive Foundation. No. BOOK, Macmilan, 1994.
[6] George Cybenko, Approximation by superpositions of a sigmoidal function, Mathematics of control, Conf. Rec. Asilomar Conf. Signals Syst. Comput. 2 (4) (1989) 303–314.
[7] Jooyoung Park, Irwin W. Sandberg, Universal approximation using radial-basis-function networks, Neural Comput. 3 (2) (1991) 246–257.
[8] V.N. Vapnik, An overview of statistical learning theory, IEEE Trans. Neural Netw. 10 (5) (1999) 988–999.
[9] Guang-Bin Huang, Qin-Yu Zhu, Chee-Kheong Siew, Extreme learning machine: theory and applications, Neurocomputing 70 (1-3) (2006) 489–501.
[10] Satish Kumar, Neural Networks: A Classroom Approach, Tata McGraw-Hill Education, 2004.
[11] Geoffrey E. Hinton, Ruslan R. Salakhutdinov, Reducing the dimensionality of data with neural networks, Science 313 (5786) (2006) 504–507.
[12] U.R. Acharya, S.V. Sree, R. Ribeiro, G. Krishnamurthi, R.T. Marinho, J. Sanches, J.S. Suri, Data mining framework for fatty liver disease classification in ultrasound: a hybrid feature extraction paradigm, Med. Phys. 39 (7Part1) (2012) 4255–4264.
[13] L. Saba, N. Dey, A.S. Ashour, S. Samanta, S.S. Nath, S. Chakraborty, J. Sanches, D. Kumar, R. Marinho, J.S. Suri, Automated stratification of liver disease in ultrasound: an online accurate feature classification paradigm, Comput. Methods Programs Biomed. 130 (2016) 118–134.
[14] V. Kuppili, M. Biswas, A. Sreekumar, H.S. Suri, L. Saba, D.R. Edla, R.T. Marinhoe, J.M. Sanches, J.S. Suri, Extreme learning machine framework for risk stratification of fatty liver disease using ultrasound tissue characterization, J. Med. Syst. 41 (10) (2017) 152.
[15] U.R. Acharya, S.V. Sree, S. Kulshreshtha, F. Molinari, J.E.W. Koh, L. Saba, J.S. Suri, GyneScan: an improved online paradigm for screening of ovarian cancer via tissue characterization, Technol. Cancer Res. Treat. 13 (6) (2014) 529–539.
[16] U.R. Acharya, M.M.R. Krishnan, L. Saba, F. Molinari, S. Guerriero, J.S. Suri, Ovarian tumor characterization using 3D ultrasound, Ovarian Neoplasm Imaging, Springer, Boston, MA, 2013, pp. 399–412.
[17] U.R. Acharya, S.V. Sree, L. Saba, F. Molinari, S. Guerriero, J.S. Suri, Ovarian tumor characterization and classification using ultrasound—a new online paradigm, J. Digit. Imaging 26 (3) (2013) 544–553.
[18] R.U. Acharya, O. Faust, A.P.C. Alvin, S.V. Sree, F. Molinari, L. Saba, A. Nicolaides, J.S. Suri, Symptomatic vs. asymptomatic plaque classification in carotid ultrasound, J. Med. Syst. 36 (3) (2012) 1861–1871.
[19] L. Saba, P.K. Jain, H.S. Suri, N. Ikeda, T. Araki, B.K. Singh, A. Nicolaides, S. Shafique, A. Gupta, J.R. Laird, J.S. Suri, Plaque tissue morphology-based stroke risk stratification using carotid ultrasound: a polling-based PCA learning paradigm, J. Med. Syst. 41 (6) (2007) 98.
[20] S. Delsanto, F. Molinari, P. Giustetto, W. Liboni, S. Badalamenti, J.S. Suri, Characterization of a completely user-independent algorithm for carotid artery segmentation in 2-D ultrasound images, IEEE Trans. Instrum. Meas. 56 (4) (2007)

1265–1274.
[21] Jasjit Suri, Luca Saba, Nilanjan Dey, Sourav Samanta, Siddhartha Sankar Nath, Sayan Chakraborty, Dinesh Kumar, João Sanches, 2083667 Online system for liver disease classification in ultrasound, Ultrasound Med. Biol. 41 (4) (2015) S18.
[22] F. Molinari, G. Zeng, J.S. Suri, Greedy technique and its validation for fusion of two segmentation paradigms leads to an accurate intima–media thickness measure in plaque carotid arterial ultrasound, J. Vasc. Ultrasound 34 (2) (2010) 63–73.
[23] L. Saba, R.S. Lippo, N. Tallapally, F. Molinari, R. Montisci, G. Mallarini, J.S. Suri, Evaluation of carotid wall thickness by using computed tomography and semi-automated ultrasonographic software, J. Vasc. Ultrasound 35 (3) (2011) 136–142.
[24] J.S. Suri, Two-dimensional fast magnetic resonance brain segmentation, IEEE Eng. Med. Biol. Mag. 20 (4) (2011) 84–95.
[25] J.S. Suri, Computer vision, pattern recognition and image processing in left ventricle segmentation: the last 50 years, Pattern Anal. Appl. 3 (3) (2000) 209–242.
[26] Liam Paninski, Jonathan Pillow, Jeremy Lewi, Statistical models for neural encoding, decoding, and optimal stimulus design, Prog. Brain Res. 165 (2007) 493–507.
[27] S. Nishimoto, A.T. Vu, T. Naselaris, Y. Benjamini, B. Yu, J.L. Gallant, Reconstructing visual experiences from brain activity evoked by natural movies, Curr. Biol. 21 (19) (2011) 1641–1646.
[28] K.N. Kay, T. Naselaris, R.J. Prenger, J.L. Gallant, Identifying natural images from human brain activity, Nature 452 (7185) (2008) 352.
[29] Anil K. Jain, Farshid Farrokhnia, Unsupervised texture segmentation using Gabor filters, Pattern Recognit. 24 (12) (1991) 1167–1186.
[30] A. Krizhevsky, I. Sutskever, G.E. Hinton, Imagenet classification with deep convolutional neural networks, Adv. Neural Inf. Process. Syst. 2012 (2012) 1097–1105.
[31] Y. LeCun, Y. Bengio, G. Hinton, Deep learning, Nature 521 (7553) (2015) 436.
[32] M.D. Zeiler, R. Fergus, Visualizing and understanding convolutional networks, European Conference on Computer Vision (2014) 818–833.
[33] Karen Simonyan, Andrew Zisserman, Very Deep Convolutional Networks for Large-Scale Image Recognition, arXiv preprint arXiv:1409.1556, 2014.
[34] C. Szegedy, W. Liu, Y. Jia, P. Sermanet, S. Reed, D. Anguelov, D. Erhan, V. Vanhoucke, A. Rabinovich, Going deeper with convolutions, Cvpr (2015).
[35] K. He, X. Zhang, S. Ren, J. Sun, Deep residual learning for image recognition, Proceedings of the IEEE Conference on Computer Vision and Pattern Recognition, (2016), pp. 770–778.
[36] J. Hu, L. Shen, G. Sun, Squeeze-and-excitation Networks, arXiv preprint arXiv:1709.01507, 2017.
[37] T. Ching, D.S. Himmelstein, B.K. Beaulieu-Jones, A.A. Kalinin, B.T. Do, G.P. Way, E. Ferrero, P.M. Agapow, M. Zietz, M.M. Hoffman, W. Xie, Opportunities and obstacles for deep learning in biology and medicine, bioRxiv (2018) 142760.
[38] Daniel L.K. Yamins, Ha Hong, Charles F. Cadieu, Ethan A. Solomon, Darren Seibert, James J. DiCarlo, Performance-optimized hierarchical models predict neural responses in higher visual cortex, Proc. Natl. Acad. Sci. 111 (23) (2014) 8619–8624.
[39] Charles F. Cadieu, Ha Hong, Daniel L.K. Yamins, Nicolas Pinto, Diego Ardila, Ethan A. Solomon, Najib J. Majaj, James J. DiCarlo, Deep neural networks rival the representation of primate IT cortex for core visual object recognition, PLoS Comput. Biol. 10 (12) (2014) e1003963.
[40] Umut Güçlü, Marcel AJ van Gerven, Deep neural networks reveal a gradient in the complexity of neural representations across the ventral stream, J. Neurosci. 35 (27) (2015) 10005–10014.
[41] Uri Hasson, Yuval Nir, Ifat Levy, Galit Fuhrmann, Rafael Malach, Intersubject synchronization of cortical activity during natural vision, Science 303 (5664) (2004) 1634–1640.
[42] Kun-Han Lu, Shao-Chin Hung, Haiguang Wen, Lauren Marussich, Zhongming Liu, Influences of high-level features, gaze, and scene transitions on the reliability of BOLD responses to natural movie stimuli, PLoS One 11 (8) (2016) e0161797.
[43] Sinno Jialin Pan, Qiang Yang, A survey on transfer learning, IEEE Trans. Knowl. Data Eng. 22 (10) (2010) 1345–1359.
[44] Yoshua Bengio, Deep learning of representations for unsupervised and transfer learning, Proceedings of ICML Workshop on Unsupervised and Transfer Learning, (2012), pp. 17–36.
[45] Grégoire Mesnil, Yann Dauphin, Xavier Glorot, Salah Rifai, Yoshua Bengio, Ian Goodfellow, Erick Lavoie, et al., Unsupervised and transfer learning challenge: a deep learning approach, Proceedings of the 2011 International Conference on Unsupervised and Transfer Learning Workshop 27 (2011) 97–111.
[46] Yi Sun, Xiaogang Wang, Xiaoou Tang, Deep learning face representation from predicting 10,000 classes, Proceedings of the IEEE Conference on Computer Vision and Pattern Recognition, (2014), pp. 1891–1898.
[47] Geert Litjens, Thijs Kooi, Babak Ehteshami Bejnordi, Arnaud Arindra Adiyoso Setio, Francesco Ciompi, Mohsen Ghafoorian, Jeroen Awm Van Der Laak, Bram Van Ginneken, Clara I. Sánchez, A survey on deep learning in medical image analysis, Med. Image Anal. 42 (2017) 60–88.
[48] Wenqing Sun, Bin Zheng, Wei Qian, Computer aided lung cancer diagnosis with deep learning algorithms, Medical Imaging 2016: Computer-Aided Diagnosis 9785 International Society for Optics and Photonics, 2016, p. 97850Z.
[49] Kai-Lung Hua, Che-Hao Hsu, Shintami Chusnul Hidayati, Wen-Huang Cheng, Yu-Jen Chen, Computer-aided classification of lung nodules on computed tomography images via deep learning technique, Oncol. Ther. 8 (2015).
[50] Fausto Milletari, Nassir Navab, Seyed-Ahmad Ahmadi, V-net: fully convolutional neural networks for volumetric medical image segmentation, 3D Vision (3DV), 2016 Fourth International Conference on (2016) 565–571.
[51] Adhish Prasoon, Kersten Petersen, Christian Igel, François Lauze, Erik Dam, Mads Nielsen, Deep feature learning for knee cartilage segmentation using a triplanar convolutional neural network, International Conference on Medical Image Computing and Computer-Assisted Intervention (2013) 246–253.
[52] Tuan Anh Ngo, Zhi Lu, Gustavo Carneiro, Combining deep learning and level set for the automated segmentation of the left ventricle of the heart from cardiac cine magnetic resonance, Med. Image Anal. 35 (2017) 159–171.
[53] Brain Leke Betechuoh, Tshilidzi Marwala, Thando Tettey, Autoencoder networks for HIV classification, Curr. Sci. (2006) 1467–1473.
[54] Qi Wei, Yinhao Ren, Rui Hou, Bibo Shi, Joseph Y. Lo, Lawrence Carin, Anomaly detection for medical images based on a one-class classification, Medical Imaging 2018: Computer-Aided Diagnosis vol. 10575, International Society for Optics and Photonics, 2018, p. 105751M.
[55] Michiel Kallenberg, Kersten Petersen, Mads Nielsen, Andrew Y. Ng, Pengfei Diao, Christian Igel, Celine M. Vachon, et al., Unsupervised deep learning applied to breast density segmentation and mammographic risk scoring, IEEE Trans. Med. Imaging 35 (5) (2016) 1322–1331.
[56] Panagiotis Korfiatis, Timothy L. Kline, Bradley J. Erickson, Automated segmentation of hyperintense regions in FLAIR MRI using deep learning, Tomography: a journal for imaging research 2 (4) (2016) 334.
[57] Richard O'Neil, Convolution operators and $ L (p, q) $ spaces, Duke Math. J. 30 (1) (1963) 129–142.
[58] Fisher Yu, Dequan Wang, Evan Shelhamer, Trevor Darrell, Deep Layer Aggregation, arXiv preprint arXiv:1707.06484, 2017.
[59] Hyeonwoo Noh, Seunghoon Hong, Bohyung Han, Learning deconvolution network for semantic segmentation, Proceedings of the IEEE International Conference on Computer Vision, (2015), pp. 1520–1528.
[60] Cheng-Yuan Liou, Wei-Chen Cheng, Jiun-Wei Liou, Daw-Ran Liou, Autoencoder for words, Neurocomputing 139 (2014) 84–96.
[61] Pascal Vincent, Hugo Larochelle, Isabelle Lajoie, Yoshua Bengio, Pierre-Antoine Manzagol, Stacked denoising autoencoders: learning useful representations in a deep network with a local denoising criterion, J. Mach. Learn. Res. 11 (December) (2010) 3371–3408.
[62] Geoffrey E. Hinton, Deep belief networks, Scholarpedia 4 (5) (2009) 5947.
[63] M. Biswas, V. Kuppili, L. Saba, D.R. Edla, H.S. Suri, E. Cuadrado-Godia, J.R. Laird, R.T. Marinhoe, J.M. Sanches, A. Nicolaides, J.S. Suri, State-of-the-art review on deep learning in medical imaging, Front. Biosci. (Landmark Ed) 1 (January (24)) (2019) 392–4264 5.
[64] Suvrit Sra, Sebastian Nowozin, Stephen J. Wright (Eds.), Optimization for Machine Learning, Mit Press, 2012.
[65] Peijun Hu, Fa Wu, Jialin Peng, Ping Liang, Dexing Kong, Automatic 3D liver segmentation based on deep learning and globally optimized surface evolution, Phys. Med. Biol. 61 (24) (2016) 8676.
[66] Wen Li, Fucang Jia, Qingmao Hu, Automatic segmentation of liver tumor in CT images with deep convolutional neural networks, J. Comput. Commun. 3 (11) (2015) 146.
[67] Jeffrey D. Browning, Lidia S. Szczepaniak, Robert Dobbins, Jay D. Horton, Jonathan C. Cohen, Scott M. Grundy, Helen H. Hobbs, Prevalence of hepatic steatosis in an urban population in the United States: impact of ethnicity, Hepatology 40 (6) (2004) 1387–1395.
[68] Mainak Biswas, Venkatanareshbabu Kuppili, Damodar Reddy Edla, Harman S. Suri, Luca Saba, Rui Tato Marinhoe, J. Miguel Sanches, Jasjit S. Suri, Symtosis: a liver ultrasound tissue characterization and risk stratification in optimized deep learning paradigm, Comput. Methods Programs Biomed. 155 (2018) 165–177.
[69] C. Szegedy, V. Vanhoucke, S. Ioffe, J. Shlens, Z. Wojna, Rethinking the inception architecture for computer vision, Proceedings of the IEEE Conference on Computer Vision and Pattern Recognition, (2016), pp. 2818–2826.
[70] Donald Lloyd-Jones, Robert J. Adams, Todd M. Brown, Mercedes Carnethon, Shifan Dai, T. Giovanni De Simone, Bruce Ferguson, et al., Heart disease and stroke statistics—2010 update, Circulation 121 (7) (2010) e46–e215.
[71] Mainak Biswas, Venkatanareshbabu Kuppili, Tadashi Araki, Damodar Reddy Edla, Elisa Cuadrado Godia, Luca Saba, Harman S. Suri, et al., Deep learning strategy for accurate carotid intima-media thickness measurement: an ultrasound study on Japanese diabetic cohort, Comput. Biol. Med. (2018).
[72] Jonathan Long, Evan Shelhamer, Trevor Darrell, Fully convolutional networks for semantic segmentation, Proceedings of the IEEE Conference on Computer Vision and Pattern Recognition, (2015), pp. 3431–3440.
[73] Anne Nielsen, Mikkel Bo Hansen, Anna Tietze, Kim Mouridsen, Prediction of tissue outcome and assessment of treatment effect in acute ischemic stroke using deep learning, Stroke 49 (6) (2018) 1394–1401.
[74] Matus Straka, Gregory W. Albers, Roland Bammer, Real-time diffusion-perfusion mismatch analysis in acute stroke, J. Magn. Reson. Imaging 32 (5) (2010) 1024–1037.
[75] Y. Song, Y.D. Zhang, X. Yan, H. Liu, M. Zhou, B. Hu, G. Yang, Computer-aided diagnosis of prostate cancer using a deep convolutional neural network from multiparametric MRI, J. Magn. Reson. Imaging (2018).
[76] Germán González, Samuel Y. Ash, Gonzalo Vegas-Sánchez-Ferrero, Jorge Onieva Onieva, Farbod N. Rahaghi, James C. Ross, Alejandro Díaz, Raúl San José Estépar, George R. Washko, Disease staging and prognosis in smokers using deep learning in chest computed tomography, Am. J. Respir. Crit. Care Med. 197 (2) (2018) 193–203.
[77] Available Online. http://www.copdgene.org/.
[78] J.ørgen Vestbo, Wayne Anderson, Harvey O. Coxson, Courtney Crim, Ffyona Dawber, Lisa Edwards, Gerry Hagan, et al., Evaluation of COPD longitudinally to identify predictive surrogate end-points (ECLIPSE), Eur. Respir. J. 31 (4) (2008) 869–873.
[79] Mariusz Bojarski, Daniel Dworakowski Davide Del Testa, Bernhard Firner, Beat Flepp, Prasoon Goyal, Lawrence D. Jackel, et al., End to End Learning for Self-

driving Cars, arXiv preprint arXiv:1604.07316, 2016.

[80] Gary Silberg, Richard Wallace, G. Matuszak, J. Plessers, C. Brower, Deepak Subramanian, Self-driving cars: the next revolution, white paper, KPMG LLP Cent. Autom. Res. (2012) 36.

[81] Luis Araujo, K. Manson, Martin Spring, Self-Driving Cars, A Case Study in Making New Markets 9 Big Innovation Centre, London, UK, 2012.

[82] S.R. Narla, The evolution of connected vehicle technology: from smart drivers to smart cars to self-driving cars, ITE J. 83 (7) (2013) 22.

[83] Casey Newton, Uber will eventually replace all its drivers with self-driving cars, Verge 5 (28) (2014) 2014.

[84] Erico Guizzo, How google's self-driving car works, IEEE Spectrum Online 18 (7) (2011) 1132–1141.

[85] Aaron M. Kessler, Elon Musk Says Self-Driving Tesla Cars will be in the us by Summer, The New York Times, 2015, p. B1.

[86] John S. Hurley, Beyond the struggle: artificial intelligence in the department of defense (DoD), ICCWS 2018 13th International Conference on Cyber Warfare and Security, (2018), p. 297.

[87] Arthur Graesser, Patrick Chipman, Frank Leeming, Suzanne Biedenbach, Deep learning and emotion in serious games, Serious Games: Mech. Effects (2009) 81–100.

[88] Seonwoo Min, Byunghan Lee, Sungroh Yoon, Deep learning in bioinformatics, Brief. Bioinf. 18 (5) (2017) 851–869.

[89] Mrutyunjaya Panda, Deep learning in bioinformatics, CSI Commun. 4 (2012).

[90] Yongjin Park, Manolis Kellis, Deep learning for regulatory genomics, Nat. Biotechnol. 33 (8) (2015) 825.

[91] Daniele Ravì, Charence Wong, Fani Deligianni, Melissa Berthelot, Javier Andreu-Perez, Benny Lo, Guang-Zhong Yang, Deep learning for health informatics, IEEE J. Biomed. Health Inform. 21 (1) (2017) 4–21.

[92] Martín Abadi, Paul Barham, Jianmin Chen, Zhifeng Chen, Andy Davis, Jeffrey Dean, Matthieu Devin, et al., TensorFlow: A System for Large-Scale Machine Learning 16 OSDI, 2016, pp. 265–283.

[93] James Bergstra, Olivier Breuleux, Frédéric Bastien, Pascal Lamblin, Razvan Pascanu, Guillaume Desjardins, Joseph Turian, David Warde-Farley, Yoshua Bengio, Theano: a CPU and GPU math compiler in python, Proc. 9th Python in Science Conf 1 (2010).

[94] Yangqing Jia, Evan Shelhamer, Jeff Donahue, Sergey Karayev, Jonathan Long, Ross Girshick, Sergio Guadarrama, Trevor Darrell, Caffe: convolutional architecture for fast feature embedding, Proceedings of the 22nd ACM International Conference on Multimedia (2014) 675–678.

[95] David Luebke, Greg Humphreys, How gpus work, Computer 40 (2) (2007).

[96] Ondirej Fialka, Martin Cadik, FFT and convolution performance in image filtering on GPU, Information Visualization, 2006. IV 2006, Tenth International Conference on (2006) 609–614.

[97] Marios Anthimopoulos, Stergios Christodoulidis, Lukas Ebner, Andreas Christe, Stavroula Mougiakakou, Lung pattern classification for interstitial lung diseases using a deep convolutional neural network, IEEE Trans. Med. Imaging 35 (5) (2016) 1207–1216.

[98] Rasool Fakoor, Faisal Ladhak, Azade Nazi, Manfred Huber, Using deep learning to enhance cancer diagnosis and classification, Proceedings of the International Conference on Machine Learning 28 (2013).

[99] Rongjian Li, Wenlu Zhang, Heung-Il Suk, Li Wang, Jiang Li, Dinggang Shen, Shuiwang Ji, Deep learning based imaging data completion for improved brain disease diagnosis, International Conference on Medical Image Computing and Computer-Assisted Intervention (2014) 305–312.

[100] Tom Brosch, Roger Tam, Alzheimer's disease neuroimaging initiative. Manifold learning of brain MRIs by deep learning, International Conference on Medical Image Computing and Computer-Assisted Intervention (2013) 633–640.

[101] Tom Brosch, Youngjin Yoo, David K.B. Li, Anthony Traboulsee, Roger Tam, Modeling the variability in brain morphology and lesion distribution in multiple sclerosis by deep learning, International Conference on Medical Image Computing and Computer-Assisted Intervention (2014) 462–469.

[102] Xiantong Zhen, Zhijie Wang, Ali Islam, Mousumi Bhaduri, Ian Chan, Shuo Li, Multi-scale deep networks and regression forests for direct bi-ventricular volume estimation, Med. Image Anal. 30 (2016) 120–129.

[103] Ezequiel Geremia, Bjoern H. Menze, Olivier Clatz, Ender Konukoglu, Antonio Criminisi, Nicholas Ayache, Spatial decision forests for MS lesion segmentation in multi-channel MR images, International Conference on Medical Image Computing and Computer-Assisted Intervention (2010) 111–118.

[104] Li Wang, Yaozong Gao, Feng Shi, Gang Li, John H. Gilmore, Weili Lin, Dinggang Shen, LINKS: learning-based multi-source IntegratioN frameworK for Segmentation of infant brain images, NeuroImage 108 (2015) 160–172.

[105] Michael Lynch, Ovidiu Ghita, Paul F. Whelan, Automatic segmentation of the left ventricle cavity and myocardium in MRI data, Comput. Biol. Med. 36 (4) (2006) 389–407.

[106] Christian Wachinger, Martin Reuter, Tassilo Klein, DeepNAT: deep convolutional neural network for segmenting neuroanatomy, NeuroImage (2017).

[107] Jelmer M. Wolterink, Tim Leiner, A. Max, Ivana I.šgum Viergever, Dilated convolutional neural networks for cardiovascular MR segmentation in congenital heart disease, Reconstruction, Segmentation, and Analysis of Medical Images (2016) 95–102.

[108] M.R. Avendi, Arash Kheradvar, Hamid Jafarkhani, A combined deep-learning and deformable-model approach to fully automatic segmentation of the left ventricle in cardiac MRI, Med. Image Anal. 30 (2016) 108–119.

[109] Mark J.J.P. van Grinsven, Bram van Ginneken, Carel B. Hoyng, Thomas Theelen, Clara I. Sánchez, Fast convolutional neural network training using selective data sampling: application to hemorrhage detection in color fundus images, IEEE Trans. Med. Imaging 35 (5) (2016) 1273–1284.

[110] Qi Dou, Hao Chen, Lequan Yu, Lei Zhao, Jing Qin, Defeng Wang, Vincent C.T. Mok, Lin Shi, Pheng-Ann Heng, Automatic detection of cerebral microbleeds from MR images via 3D convolutional neural networks, IEEE Trans. Med. Imaging 35 (5) (2016) 1182–1195.

[111] Dan C. Cireşan, Alessandro Giusti, Luca M. Gambardella, J.ürgen Schmidhuber, Mitosis detection in breast cancer histology images with deep neural networks, International Conference on Medical Image Computing and Computer-Assisted Intervention (2013) 411–418.

[112] Korsuk Sirinukunwattana, Shan E. Ahmed Raza, Yee-Wah Tsang, David R.J. Snead, Ian A. Cree, Nasir M. Rajpoot, Locality sensitive deep learning for detection and classification of nuclei in routine colon cancer histology images, IEEE Trans. Med. Imaging 35 (5) (2016) 1196–1206.

[113] Haibo Wang, Angel Cruz Roa, Ajay N. Basavanhally, Hannah L. Gilmore, Natalie Shih, Mike Feldman, John Tomaszewski, Fabio Gonzalez, Anant Madabhushi, Mitosis detection in breast cancer pathology images by combining handcrafted and convolutional neural network features, J. Med. Imaging 1 (3) (2014) 034003.

[114] Angel Cruz-Roa, Ajay Basavanhally, Fabio González, Hannah Gilmore, Michael Feldman, Shridar Ganesan, Natalie Shih, John Tomaszewski, Anant Madabhushi, Automatic detection of invasive ductal carcinoma in whole slide images with convolutional neural networks, in Medical Imaging 2014: digital pathology, Int. Soc. Opt. Photon. 9041 (2014) 904103.

[115] Holger R. Roth, Ari Seff Le Lu, Kevin M. Cherry, Joanne Hoffman, Shijun Wang, Jiamin Liu, Evrim Turkbey, Ronald M. Summers, A new 2.5 D representation for lymph node detection using random sets of deep convolutional neural network observations, International Conference on Medical Image Computing and Computer-Assisted Intervention (2014) 520–527.

[116] Dayong Wang, Aditya Khosla, Rishab Gargeya, Humayun Irshad, Andrew H. Beck, Deep Learning for Identifying Metastatic Breast Cancer, arXiv preprint arXiv:1606.05718, 2016.

[117] IBM Research Accelerating Discovery: Medical Image Analytics, 10/10/2013. Available Online. https://www.youtube.com/watch?v=0i11VCNacAE.

[118] L. Bos, Economic impact of telemedicine: a survey, Med. Care Compunet. 2 (114) (2005) 140.

[119] Available Online. https://www.wired.com/2017/01/look-x-rays-moles-living-ai-coming-job/.

[120] Computer Aided Detection Market Worth $1.9 Billion By 2022," Grand View Research, 8/2016, Available Online. http://www.grandviewresearch.com/press-release/global-computer-aided-detection-market.

[121] Charlene Liew, The future of radiology augmented with Artificial Intelligence: a strategy for success, Eur. J. Radiol. 102 (2018) 152–156.

[122] Yiftach Nagar, Thomas W. Malone, Patrick De Boer, Ana Cristina Bicharra Garcia, Essays on Collective Intelligence, PhD diss Massachusetts Institute of Technology, 2016.

[123] Michael Kremer, The O-ring theory of economic development, Q. J. Econ. 108 (3) (1993) 551–575.

[124] Available Online, https://www.enlitic.com/press-release-10272015.html.

[125] Robert E. Cooke Jr., Michael G. Gaeta, Dean M. Kaufman, John G. Henrici, Picture Archiving and Communication System, U.S. Patent 6,574,629, issued June 3, (2003).